Proton NMR Studies of Noncovalent Complexes of Cytochrome *c* Peroxidase–Cyanide with Horse and Yeast Ferricytochromes *c*†

Qian Yi,‡ James E. Erman,§ and James D. Satterlee*,‖

Department of Biochemistry and Biophysics and Department of Chemistry, Washington State University, Pullman, Washington 99164-4630, and Department of Chemistry, Northern Illinois University, DeKalb, Illinois 60115

Received May 20, 1993; Revised Manuscript Received July 28, 1993®

ABSTRACT: Noncovalent complexes of cyanide-ligated cytochrome *c* peroxidase with horse ferricytochrome *c* and yeast isozyme-1 ferricytochrome *c* have been formed in 10 mM potassium nitrate salt solutions and studied by proton NMR spectroscopy. The chemical shifts in the ferricytochrome *c* spectrum induced by complex formation with low-spin, cyanide-ligated cytochrome *c* peroxidase are similar to the corresponding shifts induced by complex formation with resting-state cytochrome *c* peroxidase, found previously. As with the resting-state enzyme, the complex between yeast cytochrome *c* and cytochrome *c* peroxidase–cyanide exhibits the larger set of complex-induced shifts. Two-dimensional proton NMR spectroscopy has been used to make resonance assignments. This was necessitated due to the extensive resonance overlap between the two proteins in the hyperfine shift region, since both heme proteins in this complex are low-spin paramagnetic species. These results expand preliminary work that revealed for the first time that cytochrome *c* binding affected the resonances of protons in the peroxidase heme pocket [Yi, Q., Erman, J. E., & Satterlee, J. D. (1992) *J. Am. Chem. Soc. 114*, 7907–7909]. The pattern of cytochrome *c* peroxidase complex-induced shifts is largely consistent with the X-ray crystal structures of these two complexes that have recently been published.

Cytochrome *c* peroxidase (CcP) catalyzes the oxidation of ferrocytochrome *c* (ferrocyt *c*) in a reaction that is believed to involve intramolecular electron transfer within a complex of the two proteins (Poulos & Kraut, 1980; Poulos & Finzel, 1984; Bosshard et al., 1991). As a result, complexes of yeast cytochrome *c* peroxidase with cytochromes *c* from various sources have been the focus of studies by many chemical and physical methods [for example, Erman and Vitello (1980), Ho et al. (1983), Bechtold and Bosshard (1985), Fishel et al. (1987), Hazzard et al. (1987, 1988), Cheung and English (1988), Wang et al. (1990), Liang et al. (1988), Kim et al. (1990), Vitello et al. (1990), Bosshard et al. (1991), McLendon (1991), Geren et al. (1991), Wallin et al. (1991), Hahm et al. (1992), Pelletier and Kraut (1992), Moench et al. (1992), Yi et al. (1992), and Corin et al. (1993)].

Interest in the CcP/cytochrome *c* complex results from the idea that the complex between the two yeast proteins represents an actual biological electron-transfer complex that is presumed to occur in the intermembrane space of yeast mitochondria. The CcP/cytochrome *c* complex serves as a paradigm for biological electron-transfer complexes in general. In addition, several properties of CcP and cytochrome *c* facilitate the study of complexes between these two proteins. The sizes of these complexes render them suitable candidates for nearly all types of spectroscopy, including NMR. The proteins are easily obtained and both proteins are water-soluble, as are the complexes, making them quite amenable to handling in either solution or the solid state.

This versatility has been an advantage in our previous solution proton NMR studies of the complexes formed between native CcP and horse, tuna, and yeast isozyme-1 (iso-1) ferricytochromes *c*. Among other things this previous NMR work revealed that the proton hyperfine shifts of ferricyt *c* were uniquely capable of directly detecting complex formation, with significant complex-induced proton NMR shifts being demonstrated by the ferricyt *c* spectra (Satterlee et al., 1987; Moench et al., 1992). It also showed that these ferricyt *c* complex-induced shift patterns were species specific. We have used these complex-induced shifts to establish the 1:1 stoichiometry of the complexes and to provide limited information on the solution structure of the complexes.

All of the previous work employed CcP in the resting state, in which the enzyme's heme iron is in the paramagnetic high-spin ferric state. Although those complexes were reasonable starting points for a comprehensive and extensive study of solution properties, using the native resting-state enzyme has two primary drawbacks. (1) The heme hyperfine-shifted resonances of resting-state CcP exhibit large line widths ($\nu_{1/2} \approx 1000$ Hz at 360 MHz), making it very difficult to reproducibly detect possible complex-induced effects on CcP. (2) The complexes that we have studied so far have been characterized as "product" complexes, in the sense that a complex of the resting-state enzyme and ferricyt *c* is what results from the final electron-transfer step in CcP's proposed catalytic cycle (Bosshard et al., 1991; Yi et al., 1993). However, the spontaneous reaction of the active-intermediate complexes, consisting of a CcP oxidized intermediate (with a low-spin ferryl heme) and reduced (i.e., ferrous) cyt *c*, precludes their study by solution-state NMR (Yi et al., 1993).

Here we present data from a set of complexes in which we have used a low-spin cyano form of the resting enzyme, CcPCN, in order to approximate the heme ligation state of the enzymatic ferryl CcP intermediates (i.e., compounds I and II). Noncovalent CcPCN complexes with both horse and yeast iso-1 ferricyt *c* have been studied by one- and two-

† This work was supported by a grant from the National Institutes of Health (GM45986). NMR spectrometer acquisition was supported by NIH Grant RR06314.

* Corresponding author.

‡ Department of Biochemistry and Biophysics, Washington State University.

§ Department of Chemistry, Northern Illinois University.

‖ Department of Chemistry, Washington State University.

® Abstract published in *Advance ACS Abstracts*, October 1, 1993.

0006-2960/93/0432-10988$04.00/0

dimensional proton NMR spectroscopy. This work complements our previously published work with resting-state CcP (Moench et al., 1992). Use of CcPCN, which is a structural analog for the oxidized, ferryl enzyme intermediate, CcP compound II, has several advantages over resting-state CcP. CcPCN, like CcP compound II, is low-spin with a six-coordinate heme iron ion, although the oxidation state of the heme iron ion is one equivalent lower than that found in compound II. One distinct advantage of CcPCN over CcP is that CcPCN displays resolved proton hyperfine shifts due to active-site amino acids as well as the heme. In addition, because the CcPCN hyperfine resonances are relatively narrow ($\nu_{1/2} \approx 100$ Hz at 500 MHz), we have been able to document complex-induced shifts in CcPCN as well as in the ferricytochromes *c*.

EXPERIMENTAL PROCEDURES

Both horse and yeast iso-1 cytochromes *c* were purchased from Sigma Chemical Co. Horse cytochrome *c* was in the oxidized form as judged by UV–visible spectroscopy and was used without further purification. Yeast iso-1 cytochrome *c*, which contains some reduced forms in the commercial preparation, was oxidized completely with $K_3Fe(CN)_6$ (Baker Analyzed). The excess $K_3Fe(CN)_6$ was removed by passing the oxidized iso-1 through a short Dowex 8× (Bio-Rad) column prior to use. Additional protocols for handling the proteins and formation of the complexes closely followed those previously described (Moench et al., 1992). Methods for handling native yeast iso-1 cytochrome *c* followed those previously described (Moench & Satterlee, 1989). Cytochrome *c* peroxidase was isolated and purified as previously described (Erman & Vitello, 1980; Vitello et al., 1990). Protein concentrations were measured by visible spectroscopy using extinction coefficients of 106 mM^{-1} cm^{-1} at 409 nm for all ferricytochromes *c*, 93 mM^{-1} cm^{-1} at 408 nm for native, resting state CcP, and 103 mM^{-1} cm^{-1} at 414 nm for CcPCN. All protein solutions for NMR spectroscopy were made up in a standard, uniform solution consisting of 10 mM KNO_3 in D_2O (99.9%; Isotec), pH′ 6.5. pH′ refers to the uncorrected meter reading in this D_2O solution using a Fisher 910 meter and a calibrated combination electrode. The pH was adjusted, where necessary, using diluted DCl (MSD Isotopes).

Proton homonuclear two- and one-dimensional NMR experiments were run on a Varian VXR500 operating at the nominal frequency of 500 MHz. The calibrated probe temperature was regulated at 20 °C. The residual water resonance was used as an internal reference and assigned a chemical shift of 4.70 ppm. Suppression of the residual solvent resonance was achieved by irradiation at all times except during acquisition. Typical 1D acquisition parameters were a 60 kHz spectral width described by 33K data points in experiments that used a recycle time of 0.57 s. Homonuclear proton NOESY and COSY experiments were performed using the standard library programs as previously described (Satterlee et al., 1991; Satterlee & Erman, 1991). Typical data matrices were collected that consisted of 4096 × 256 hypercomplex points, and were processed to final sizes that were 4K × 4K using either sine-bell or sine-squared apodization. Buildup of the nuclear Overhauser effect was measured directly from intensities of resonances in slices taken from the NOESY experiment. Within a given set of NOESY experiments, in which the mixing times were randomly varied, all instrumental parameters remained constant, rendering the curves, such as those shown in Figure 5, internally self-consistent. The significance of the complex-induced shifts reported in Table I was estimated using the *t*-test.

Table I: Proton Resonance Assignments and Chemical Shift Comparisons of CcPCN/Yeast Iso-1 Ferricyt *c* and CcPCN/Horse Ferricyt *c* Complexes with Free CcPCN and Ferricytochromes *c*[a]

resonance CcPCN	CcPCN/horse cyt *c*			CcPCN/yeast iso-1 cyt *c*		
	free	complex	Δ (Hz)[b]	free	complex	Δ (Hz)
heme 3-CH_3	30.98	30.95	−14	30.98	30.81	−83
heme 8-CH_3	27.91	27.87	−19	27.91	27.37	−273
His175β	19.84	19.79	−24	19.84	19.86	10
His175β'	15.06	15.00	−27	15.06	15.26[c]	98
His175NpH	13.03	13.00	−15	13.03	13.06	14
heme 4α	15.93	15.89	−19	15.93	15.54[c]	−190
heme 4β	−2.25	−2.27	−11	−2.25	−2.19[c]	−29
heme 4β'	−4.02	−4.05	−15	−4.02	−4.21	−93
heme 7α	18.45	18.58	67	18.45	18.44	−5
heme 7β	−1.56	−1.56	−1	−1.56	−1.63	−32
His52C2H	14.18	14.19	5	14.18	14.22	24

resonance ferricyt *c*	CcPCN/horse cyt *c*			CcPCN/iso-1 cyt *c*		
	free	complex	Δ (Hz)[b]	free	complex	Δ (Hz)
heme 8-CH_3	36.04	35.56	−239	35.69	35.98	146
heme 3-CH_3	32.91	33.69	390	32.12	34.25	1065
heme 7α	19.33	18.74	−298	16.27	15.54[c]	−361
heme 7α'	11.32	11.31	−5	12.95	13.54	298
His18β	14.68	14.66	−14	15.34	15.42[c]	40
Met80β	12.84	12.79	−24	12.46	11.80	−327
Met80ϵ	−25.13	−25.06	34	−24.01	−23.43	291
Pro30δ	−2.77	−2.74	14	−1.83	−1.62	102
Pro30δ'	−6.86	−6.79	31	−6.08	−5.45	314
Leu68δ	−3.02	−3.02	0	−3.56	−3.94	−185
Phe82ϕ	5.77[c]	5.91[c]	71	5.90[c]	6.10[c]	98
4β-CH_3	2.87[c]	2.98[c]	52	2.62[c]	2.70[c]	42

[a] H_2O resonance (4.70 ppm) was used as the internal chemical shift reference. All data are reported at 20 °C in 10 mM KNO_3/D_2O (pH′ 6.5). [b] Low-frequency (upfield) complex-induced shifts ($\Delta = \delta_{complex} - \delta_{free}$) are denoted by a negative sign. Shifts greater than 36 Hz are statistically significant at the 95% confidence level. [c] Chemical shift obtained from two-dimensional NOESY spectra.

Models of CcP were created on a Silicon Graphics Iris workstation using the program Quanta (Polygen) from the refined coordinates (Finzel et al., 1984) deposited in the Protein Data Bank (Bernstein et al., 1977).

RESULTS AND DISCUSSION

Spectra of the Individual Proteins and the Complexes. Both CcPCN and ferricytochrome *c* are low-spin ferriheme proteins. Their hyperfine shift patterns reflect the combination of contact and pseudocontact effects characteristic of six-coordinate ferriheme proteins (Satterlee, 1986), and unlike previous results (Satterlee et al., 1987; Moench et al., 1992) where the total resonance dispersion was ~130 ppm, here it is only ~68 ppm. This situation is shown in Figures 1 and 2.

Figure 1 presents the 500-MHz proton spectra of yeast isozyme-1 (iso-1) ferricytochrome *c*, CcPCN, and an equimolar mixture of the two proteins. As a reference for the following discussion, Figure 1 also presents the labeled structures of the heme and its ligands in CcPCN and ferricyt *c*. As described in the figure caption, all solution conditions were identical for each of the NMR samples shown in Figure 1, including the low salt concentrations necessary to facilitate complex formation. One can see by comparing the spectra that spectrum C reflects complex formation by the observed shift differences compared to the individual proteins (the complex-induced shift), as well as by line-width increases (Satterlee et al., 1987). These complex-induced shifts are quantitatively presented in Table I, along with their resonance assignments. Either Figure 1 or Table I reveals that significant complex-induced proton resonance shifts occur for both proteins. This observation was previously reported for the heme methyl resonances of

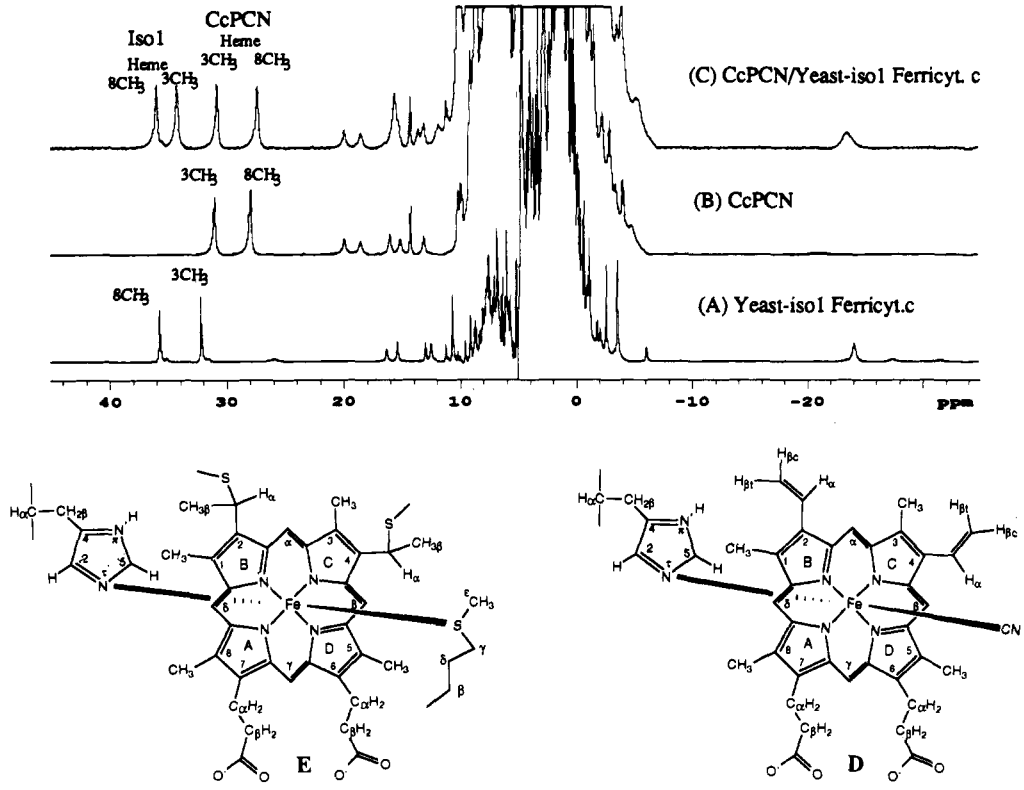

FIGURE 1: (A–C) 500-MHz one-dimensional ^1H NMR spectra of the 1:1 CcPCN/yeast iso-1 ferricyt *c* complex and individual proteins. All of the samples were in 10 mM KNO_3/D_2O (pH′ 6.5), and the spectra were obtained at 20 °C. (D) Heme and ligands for CcPCN. (E) Heme and ligands for yeast iso-1 ferricytochrome *c*.

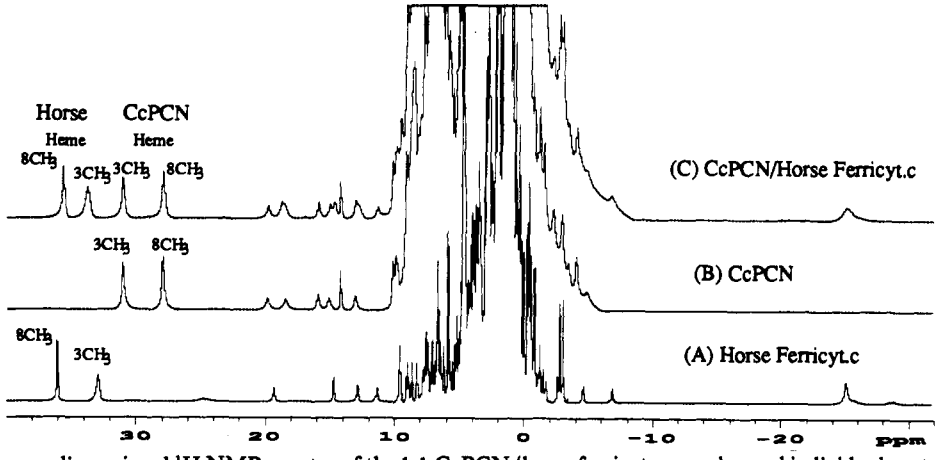

FIGURE 2: 500-MHz one-dimensional ^1H NMR spectra of the 1:1 CcPCN/horse ferricyt *c* complex and individual proteins. All of the samples were in 10 mM KNO_3/D_2O (pH′ 6.5), and spectra were obtained at 20 °C.

each protein (Yi et al., 1992) and was the first experimental observation that complex formation could alter the observed proton shifts of the CcPCN heme. From the more recent, additional data presented here, it is clear that several other resolved hyperfine resonances in both the high-frequency and low-frequency hyperfine shift regions also experience complex-induced shifts. As shown later, the pattern of complex-induced shifts supports a solution structure for the CcPCN/yeast ferricyt *c* complex similar to the recently reported solid-state crystal structure (Pelletier & Kraut, 1992).

A similar set of spectra is shown in Figure 2 for CcPCN and horse ferricytochrome *c*, with the the resonance assignments and hyperfine resonance shifts also reported in Table I.

Resonance Assignments for the Complexes. One of the problems associated with the lower hyperfine shift dispersion encountered when two low-spin ferriheme proteins form complexes is that both of these proteins display similar spectra in the same spectral regions. This leads to significant resonance overlap, as demonstrated in Figures 1C and 2C, particularly in the high-frequency region between 10 and 20 ppm. This complicates identification of individual resonances and accurate determination of their complex-induced shifts. Two-dimensional proton homonuclear NOESY and MCOSY experiments have enabled us to make unambiguous hyperfine resonance assignments and to determine the complex-induced shifts to a reproducibility of ±0.02 ppm (±10 Hz) at 500 MHz. Examples of these results are given by Figures 3 and 4. Figure 3 presents the NOESY spectrum of the CcPCN/yeast iso-1 ferricyt *c* 1:1 complex with some of the assignments labeled. Figure 4 presents the same data for the CcPCN/horse ferricyt *c* 1:1 complex.

There are several important points to be made about the two-dimensional spectra. (1) As these results show, high-quality two- dimensional proton NMR spectra can be obtained

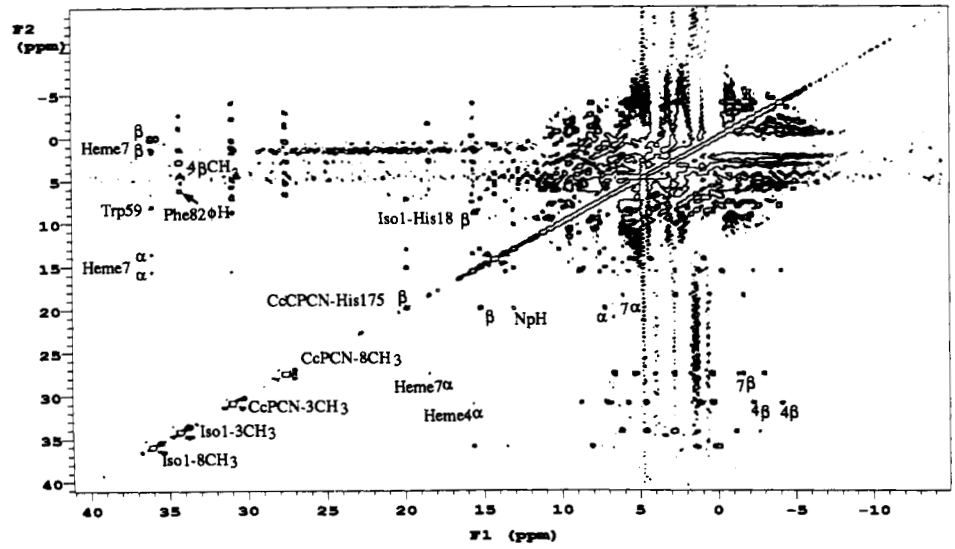

FIGURE 3: Proton homonuclear NOESY spectrum of the CcPCN/yeast iso-1 ferricyt *c* 1:1 complex in 10 mM KNO_3/D_2O (pH′ 6.5) at 20 °C (mixing time 30 ms). Cytochrome *c* assignments are shown above the diagonal, and CcPCN assignments are shown below the diagonal.

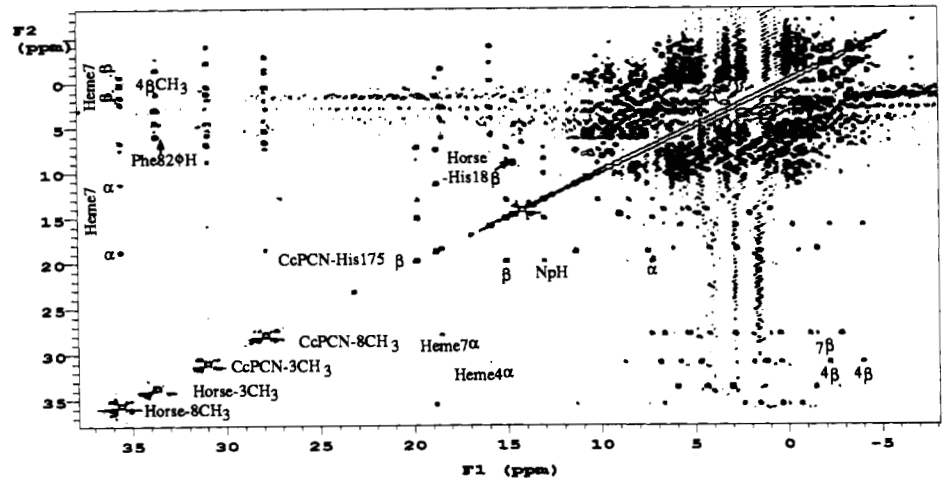

FIGURE 4: Proton homonuclear NOESY spectrum of the 1:1 CcPCN/horse ferricyt *c* complex in 10 mM KNO_3/D_2O (pH′ 6.5) at 20 °C (mixing time 30 ms). Cytochrome *c* assignments are shown above the diagonal, and CcPCN assignments are shown below the diagonal.

on M_r = ~47 000 complexes. Although the NOESY data were excellent, the MCOSY spectra were less satisfactory, with only two cross peaks detected between strongly hyperfine-shifted resonances (not shown). (2) The NOESY results were achieved using a very short total recycle time, with a repetition rate of 3.0 s^{-1}. This fast recycle rate was allowed by the fact that the NOEs in complexes of this size reach maximum values at quite short mixing times, as shown by the NOE buildup curves for representative resonances in Figure 5. (3) Resolution and assignment of overlapping resonances (Figures 1 and 2) are achievable by virtue of the second spectral dimension. (4) With the NOE connectivity patterns of the individual proteins as a guide (Satterlee & Moench, 1987; Moench & Satterlee, 1989; Santos & Turner, 1987; Moench et al., 1991; Satterlee & Erman, 1991), it was easy to recognize NOE connectivities in the spectrum of each complex, which led to straightforward resonance assignments.

Stoichiometry of the Complexes. It is clear from the data presented in Figures 1 and 2 and Table I that significant complex-induced proton NMR shifts occur in 1:1 mixtures of CcPCN and each of the ferricytochromes *c* when the solution salt concentration is low (10 mM). This behavior is definitive for complex formation, as similar work on the complexes of these same cytochromes *c* with the resting-state enzyme CcP have shown (Satterlee et al., 1987; Moench et al., 1992). In

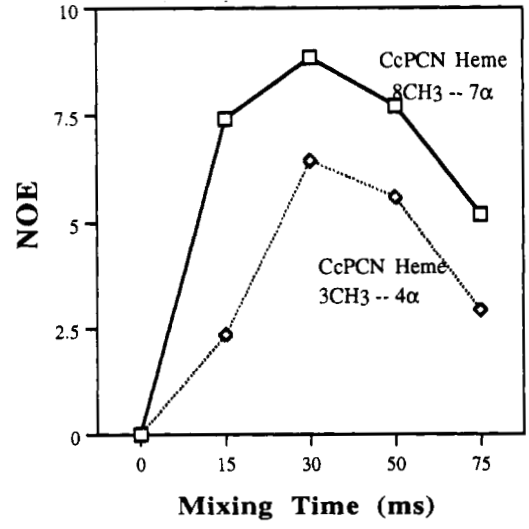

FIGURE 5: NOE buildup curves of proton cross peaks in two-dimensional NOESY spectra of the CcPCN/yeast iso-1 complex. Solution conditions were identical to those given for Figure 3.

Figures 1 and 2 and Table I, we have presented data for the 1:1 complexes because the following results indicate that the stoichiometry of both complexes is 1:1.

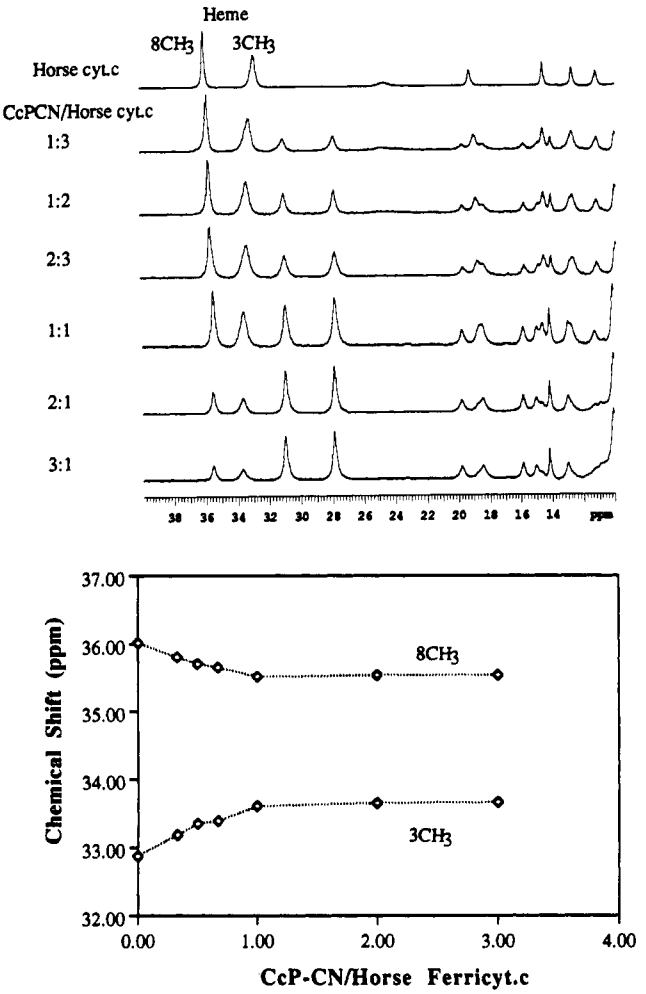

FIGURE 6: Stoichiometry of the CcPCN/horse ferricyt *c* complex as demonstrated by heme methyl group shift changes as a function of protein mole ratio in a protein titration experiment: (A, top) 500-MHz proton spectra; (B, bottom) graph of shift data showing the slope change at a 1:1 ratio. The total protein concentration was held constant at 1 mM and the solution conditions were identical to those given for Figure 4.

Complex with Horse Ferricytochrome c. For horse ferricyt *c*, many of the resolved hyperfine-shifted resonances change position smoothly as the concentration of CcPCN is increased relative to that of cyt *c*, as shown in Figure 6A. The reverse is also true; CcPCN resonances change position as the relative concentration of horse ferricyt *c* is increased. This behavior is the same as that in titrations of similar stoichiometry in which resting-state CcP was used (Satterlee et al., 1987), and it is known from that work that plots such as Figure 6B reveal the stoichiometry of the complexes from the break-point in the data. Just as for the analogous complex formed using resting-state CcP, the results here indicate that the CcPCN/horse ferricyt *c* complex has 1:1 stoichiometry under these conditions.

Complex with Yeast Isozyme-1 Ferricytochrome c. The heme 3-methyl resonance in yeast iso-1 ferricytochrome *c* experiences the largest complex-induced shift of any resolved resonance in this complex. The shift is so large that, as shown in Figure 7, individual heme 3-CH_3 resonances of the free iso-1 and the CcPCN-bound iso-1 can be observed simultaneously when the total concentration of iso-1 ferricyt *c* exceeds the CcPCN concentration. In experiments like that depicted in Figure 7, assignment of the free-form ferricyt *c* 3-CH_3 was made by comparison with the spectrum of a solution of iso-1 ferricyt *c* alone under identical solution conditions. When

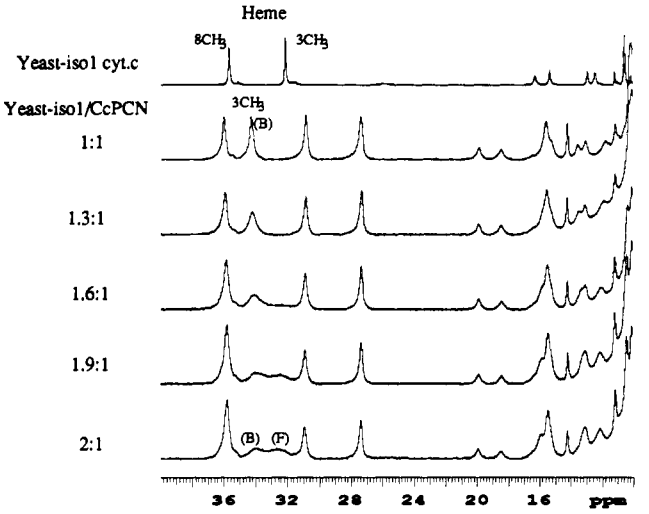

FIGURE 7: Stoichiometry of the CcPCN/yeast iso-1 ferricyt *c* complex as demonstrated by a protein titration experiment. Solution conditions were identical to those given for Figure 3. Labels B and F refer to peaks from the CcPCN-bound and free forms of cytochrome *c*, respectively.

the CcPCN concentration is equal to, or in excess of, the iso-1 ferricyt *c* concentration, only iso-1 resonances characteristic of the bound form are observed. Again, this behavior parallels that observed in the iso-1 ferricyt *c* complex with resting-state CcP (Moench et al., 1992). The data in Figure 7 clearly establish the stoichiometry of the CcPCN/yeast iso-1 ferricyt *c* complex as 1:1 under these conditions.

Analysis of the Complex-Induced Shifts (Table I). An analysis of the data presented in Table 1 includes the following main points.

(1) The magnitudes of the complex-induced shifts reported in Table I for the CcPCN/yeast iso-1 complex are generally much larger than those for the CcPCN/horse complex. Similar results were found in the corresponding complexes involving resting-state CcP (Moench et al., 1992), and as in those cases, it is also obvious here that the complex of the physiological partner proteins (yeast CcPCN/yeast cyt *c*) is different from the other complex. From the previous data on resting-state CcP complexes (Moench et al., 1992), we suggested that this was due to the formation of a more intimate complex between the physiological redox partners, and this speculation was recently borne out by the published crystal structures of these two complexes (Pelletier & Kraut, 1992). As a result of the data in Table I, we suggest that in the CcPCN complexes studied here the physiological partners again form a more intimate complex in comparison to the complex with horse ferricytochrome *c*.

(2) For the ferricyt *c* data presented here, it is clear from the similarity of these complex-induced shifts to those in the corresponding complexes with resting-state CcP (Moench et al., 1992) that the magnetic environment of either species of ferricyt *c* in a complex is independent of the CcP axial ligation and spin state. This implies that CcPCN/yeast iso-1 ferricyt *c* and CcP/yeast iso-1 ferricyt *c* complexes have indistinguishable solution structures and a similar conclusion for the corresponding horse ferricyt *c* complexes.

(3) In both of these complexes (CcPCN/yeast iso-1 ferricyt *c* and CcPCN/horse ferricyt *c*), the ferricytochrome *c* heme 3-methyl resonance displays the largest complex-induced shift of any of the resolved hyperfine-shifted resonances. In fact, a complex-induced shift of over 2 ppm is observed for the heme 3-methyl resonance of yeast iso-1 ferricyt *c*. These results indicate that the heme 3-methyl group of each ferricyt *c* must

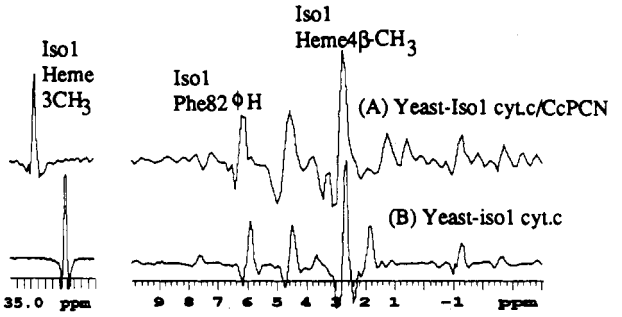

FIGURE 8: One-dimensional spectrum slices taken from proton homonuclear two-dimensional NOESY spectra of the CcPCN/yeast iso-1 ferricyt *c* complex and individual yeast iso-1 ferricyt *c*. Solution conditions were identical to those given for Figure 3.

be an integral part of the protein/protein interface in solution. Very similar results were found for the resting-state CcP complexes (Satterlee et al., 1986; Moench et al., 1992).

(4) In contrast to the large ferricyt *c* heme 3-methyl resonance shifts, complex formation induces only very small shifts in the protons of the other heme pyrrole ring C substituent in the ferricytochromes *c*. Even in yeast iso-1, where the largest shifts are generally expected, only very slight complex-induced shifts are observed for the heme 4β-CH_3 (the CBC methyl; Pelletier & Kraut, 1992), and these are comparable to those found in the CcPCN/horse ferricyt *c* complex. This difference is striking, and it can be readily seen when the same slices in comparable NOESY spectra for yeast iso-1 ferricyt *c* in the complex and free in solution are compared under identical conditions, as in Figure 8. Each slice is taken through the respective (diagonal) iso-1 3-CH_3 resonance, and each represents NOEs connected to the heme 3-CH_3. We have previously shown that NOE connectivities to the heme 3-CH_3 in ferricytochromes *c* include the heme 4β-CH_3 and the Phe82 protons (Moench et al., 1992; Moench & Satterlee, 1989). In contrast to the large 3-CH_3 complex-induced shift shown in Figure 8, the iso-1 4β-CH_3 and Phe82 complex-induced shifts are very small, although they are similar to those found in the corresponding resting CcP complex. Similar results are found for the CcPCN/horse ferricyt *c* complex (Table 1).

(5) Compared to the largest ferricyt *c* shifts, the complex-induced shifts for CcPCN hyperfine-shifted resonances are smaller, but still significant. The lower magnitude of these shifts is not unexpected in view of the buried nature of the heme active site in CcP (Kraut, 1981; Finzel et al., 1984). In this context, we judge it noteworthy to have found any complex-induced shifts whatsoever, particularly for the resonances of the His175 protons, which are located in the heme active site. We can infer that these complex-induced shifts for CcPCN active-site protons must reflect a local structural rearrangement on the proximal side of the heme that occurs as a result of ferricyt *c* binding. Ferricytochrome *c* binding is thus communicated to the CcPCN active site, which raises the interesting question of whether the structural changes so caused may be a "triggering signal" for electron transfer.

SUMMARY

We have demonstrated here that complex formation induces significant changes in the proton NMR spectra of CcPCN, horse ferricyt *c* and yeast isozyme-1 ferricyt *c*. In the case of the ferricytochromes *c*, the results are similar to those found in complexes with resting-state CcP. What is significant, however, is that these experimental results reveal that ferricyt *c* binding is transmitted to the heme active site of CcPCN.

The pattern of complex-induced shifts reported here is generally consistent with the published solution-state structure of each of the complexes (CcP/horse cyt *c* and CcP/yeast iso-1 cyt *c*) (Pelletier & Kraut, 1992). In this regard, it is notable that, in the CcPCN/yeast iso-1 complex, the statistically significant complex-induced CcPCN NMR shifts are from protons of the proximal histidine, the heme pyrrole C substituents (heme 4-vinyl and heme 3-methyl), and the heme pyrrole A substituents (primarily the 8-methyl). This pattern is consistent with the crystal structure of the complex, as follows. A complex-induced shift in the His175 protons likely reflects a structural rearrangement propagated along the "heme connecting" segment of the polypeptide that was identified by Pelletier and Kraut (1992). This segment in CcP consists of [His175], Trp191, Gly192, Ala193, and Ala194 and is the shortest link between the CcP heme and the iso-1 cytochrome *c* heme. The large CcPCN 8-CH_3 proton shift is thus a result of two factors. (1) Judging from the published structure of the complex, the 8-CH_3 group lies close to the protein/protein interface so that ferricyt *c* binding could have a direct impact on its magnetic environment. (2) The refined CcP crystal structure (Finzel et al., 1984) shows that Trp191 (part of the heme connecting segment) lies within van der Waals distance from heme pyrrole A and virtually touches the CcPCN 8-CH_3, leading to the suggestion that the primary complex-induced effect may be the result of a structural rearrangement propagated from the iso-1 ferricyt *c* binding site along the heme connecting segment to the CcPCN heme. For both possibilities, the result could be subsequently transmitted across the CcPCN heme to the pyrrole C substituents (4-vinyl, 3-methyl) via an electronic effect that results from the spatial relationship of the heme eπ orbitals that contain the delocalized unpaired electron density (La Mar & Walker, 1978; Gouterman, 1978). This concept has been used to understand the pairwise complex-induced shifts of the ferricyt *c* heme methyls (Satterlee et al., 1987).

In contrast, none of the resonances assigned to the distal, catalytically implicated amino acids (W51, H52, R48) so far exhibit complex-induced shifts, thereby indicating no net changes in the magnetic environment for resolved protons of these amino acids. We may infer from this result that there are no detectable structural changes in this region of CcPCN that occur as a consequence of ferricyt *c* binding. These NMR data are, therefore, consistent not only with the relative positioning of the two proteins in each complex, as described in the X-ray structures, but also with the ideas recently put forth concerning the involvement of the protein region proximal to the heme in an electron-transfer pathway (Pelletier & Kraut, 1992; Beratan et al., 1992).

These solution data, as with previous solution NMR work on complexes of the resting-state CcP (Satterlee et al., 1987; Moench et al., 1992), strongly implicate the ferricyt *c* heme pyrrole C in the protein/protein interface. This is consistent with the crystal structures of the related horse and yeast iso-1 ferricyt *c* complexes with resting-state CcP (Pelletier & Karut, 1992). The pattern of ferricyt *c* complex-induced shifts observed for the ferricytochrome *c* complexes with CcPCN elucidated in this work, and the similar pattern found for corresponding ferricytochrome *c* complexes with CcP (Moench et al., 1992), however, suggests that a slightly different interfacial orientation of the complex partner proteins may occur in solution compared to the crystal. The bases for this suggestion are the NMR results which show that, in each of the six complexes studied so far in solution, the ferricyt *c* heme 3-CH_3 resonance exhibits the largest complex-induced

shifts. In each case, those complex-induced shifts are far larger than those found for the the heme 4β-CH_3 (CBC methyl; Pelletier & Kraut, 1992), which is the other heme C substituent. Furthermore, in each of these six complexes the complex-induced heme 4β-CH_3 proton resonance shift is comparable in magnitude and direction. Unlike the heme 3-CH_3 peak, the complex-induced shift of the heme 4β-CH_3 resonance in each of these complexes does not discriminate between the complex of the physiological partners and the complex of the nonphysiological partners. These results specifically indicate to us that, for both of the CcPCN complexes studied here, the change in magnetic environment (and, hence, we infer structural environment) experienced by each 4β-CH_3 is identical, whereas for the heme 3-CH_3 it is not.

Another piece of information possibly relevant to refining the solution structure of the CcPCN/iso-1 ferricyt *c* complex is found in Figure 8. The NOESY slice of the complex (trace A) displays one additional off-diagonal peak at 0.6 ppm that is not found in the corresponding slice of the cytochrome *c* alone (trace B). It is probable that this extra cross peak represents an intermolecular NOE between the iso-1 ferricyt *c* and a group on CcPCN. It is interesting to note that the peak position (0.6 ppm) is consistent with that of an alanine methyl group. When combined with the crystal structure of the complex, it seems likely that this could be either Ala193 or Ala194 on CcPCN. A similar "extra" NOE was found in the one-dimensional NOE spectrum of the corresponding complex of the resting-state enzyme (Moench et al., 1992), which would reinforce the essential similarity of these complexes. A detailed investigation of potential intermolecular NOEs in these complexes is now in progress; however, in summary, the currently available NMR data suggest that, in the solution structure of the CcP and CcPCN complexes with ferricytochromes *c*, the ferricyt *c* heme 3-CH_3 is in more direct contact with CcP than is apparently shown in the crystal structure (Pelletier & Kraut, 1992).

REFERENCES

Bechtold, R., & Bosshard, H. R. (1985) *J. Biol. Chem. 260*, 5191–5200.

Beratan, D. N., Onuchic, J. N., Winkler, J. R., & Gray, H. B. (1992) *Science 258*, 1740–1741.

Bernstein, F. C., Koetzle, T. F., Williams, G. J. B., Meyer, E. F., Jr., Brice, M. D., Rodgers, J. R., Kennard, O., Shimanouchi, & Tasumi, M. (1977) *J. Mol. Biol. 112*, 535–542.

Bosshard, H. R., Anni, H., & Yonetani, T. (1991) *Peroxidases in Chemistry and Biology* (Everse, J., Everse, K. & Grisham, M. B., Eds.) Vol. 2, pp 51–83, CRC Press, Boca Raton, FL.

Cheung, E., & English, A. M. (1988) *Inorg. Chem. 27*, 1078–1081.

Corin, A. F., Hake, R. A., McLendon, G., Hazzard, J. T., & Tollin, G. (1993) *Biochemistry 32*, 2756–2762.

Erman, J. E., & Vitello, L. B. (1980) *J. Biol. Chem. 255*, 6224–6337.

Finzel, B. C., Poulos, T. L., & Kraut, J. (1984) *J. Biol. Chem. 259*, 13027–13036.

Fishel, L. A., Villafranca, J. E., Mauro, J. M., & Kraut, J. (1987) *Biochemistry 26*, 351–360.

Geren, l., Hahm, S., Durham, B., & Millett, F. (1991) *Biochemistry 30*, 9450–9457.

Gouterman, M. (1978) *The Porphyrins* (Dolphin, D., Ed.) Vol. iii, pp 1–165, Academic Press, New York.

Hahm, S., Durham, B., & Millett, F. (1992) *Biochemistry 31*, 3472-3477.

Hazzard, J. T., Poulos, T. L., & Tollin, G. (1987) *Biochemistry 26*, 2836–2848.

Hazzard, J. T., McLendon, G., Cusanovich, M. A., Das, G., Sherman, F., & Tollin, G. (1988) *Biochemistry 27*, 4445–4451.

Ho, P. S., Hoffman, B. M., Kang, C. H., & Margoliash, E. (1983) *J. Biol. Chem. 258*, 4356–4363.

Kim, K. L., Kang, D. S., Vitello, L. B., & Erman, J. E. (1990) *Biochemistry 29*, 9150–9159.

Kraut, J. (1981) *Biochem. Soc. Trans. 9*, 197–202.

La Mar, G. N., & Walker, F. A. (1978) *The Porphyrins* (Dolphin, D., Ed.) Vol. iv, pp 61–157, Academic Press, New York.

Liang, N., Mauk, A. G., Pielak, G. J., Johnson, J. A., Smith, M., & Hoffman, B. M. (1988) *Science 240*, 311–313.

McLendon, G. (1991) *Struct. Bonding 75*, 159–176

Moench, S. J., & Satterlee, J. D. (1989) *J. Biol. Chem. 264*, 9923–9931.

Moench, S. J., Shi, T. M., & Satterlee (1991) *J. Biol. Chem. 264*, 9923-9931.

Moench, S. J., Chroni, S., Lou, B. S., Erman, J. E., & Satterlee, J. D. (1992) *Biochemistry 31*, 3661–3670.

Pelletier, H., & Kraut, J. (1992) *Science 258*, 1748–1755.

Poulos, T. L., & Kraut, J. (1980) *J. Biol. Chem. 255*, 10322–10330.

Poulos, T. L., & Finzel, B. C. (1984) *Pept. Protein Rev. 4*, 115–171.

Santos, H., & Turner, D. L. (1987) *FEBS Lett. 226*, 179–184.

Satterlee, J. D. (1986) *Annual Reports on NMR Spectroscopy* (Webb, G. A., Ed.) Vol. 17, pp 79–178, Academic Press, London.

Satterlee, J. D., & Moench, S. J. (1987) *Biophys. J.52*, 101–107.

Satterlee, J. D., & Erman, J. E. (1991) *Biochemistry 30*, 4398–4405.

Satterlee, J. D. Moench, S. J., & Erman, J. E. (1987) *Biochim. Biophys. Acta 912*, 87–97.

Satterlee, J. D., Russell, D. J., & Erman, J. E. (1991) *Biochemistry 30*, 9072–9077.

Vitello, L. B., Huang, M., & Erman, J. E. (1990) *Biochemistry 29*, 4283–4288.

Wallin, S. A., Stemp, E. D. A., Everest, A. M., Nocek, J. M., Netzel., T. L., & Hoffman, B. M. (1991) *J. Am. Chem. Soc. 113*, 1842–1844.

Wang, J., Mauro, J. M., Edwards, S. L., Oatley, S. J., Fishel, L. A., Ashford, V. A., Xuong, N., & Kraut, J. (1990) *Biochemistry 29*, 7160–7173.

Yi, Q., Erman, J. E., & Satterlee, J. D. (1992) *J. Am. Chem. Soc. 114*, 7907–7909.

Yi, Q., Alam, S., Satterlee, J. D., & Erman, J. E. (1993) *Techniques in Protein Chemistry IV* (Angelotti-Hogue, R., Ed.) 605–613.